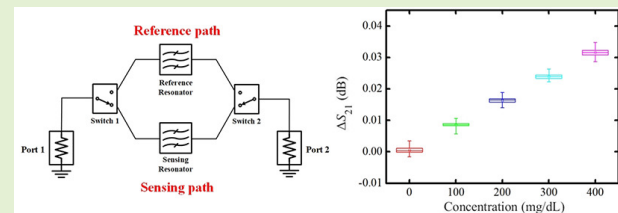


Non-Invasive Fluidic Glucose Detection Based on Dual Microwave Complementary Split Ring Resonators With a Switching Circuit for Environmental Effect Elimination

Chorom Jang¹, Student Member, IEEE, Jin-Kwan Park¹, Student Member, IEEE, Hee-Jo Lee², Member, IEEE, Gi-Ho Yun, and Jong-Gwan Yook¹, Senior Member, IEEE

Abstract—In this paper, a microwave fluidic glucose sensor based on dual complementary split ring resonators (CSRRs) with a switching circuit is proposed for non-invasive and continuous glucose concentration detection. A CSRR has been designed to detect subtle changes in the dielectric constant of glucose solutions, and the electric field distribution is utilized to determine the effective sensing region. In a well-controlled environment, the glucose concentration can be detected by tracking the transmission coefficient of the designed CSRR. However, because the variations in dielectric constant with the glucose concentration are very small, the environmental factors (i.e., ambient temperature and relative humidity) can be dominant compared to the glucose concentration. To qualify the effect of the environmental factors, the variation in the transmission coefficient of the CSRR has been measured when the ambient temperature condition is varied from 293 K to 313 K and the relative humidity is varied from 30% to 90% inside temperature- and humidity-controlled chamber. Moreover, the environmental effects are calibrated out using two identical CSRRs with the switching circuit: one detects changes in the glucose concentration, while the other operates as a reference for environmental factors. After the elimination of the environmental effects, glucose concentrations in the range of 0 mg/dL to 400 mg/dL have been measured, and the sensitivity is 0.008dB/(100mg/dL). In addition, the reproducibility of the proposed sensor is verified by repeated measurements. It is demonstrated that the proposed sensor can detect glucose concentrations under practical environmental conditions.

Index Terms—Glucose sensor, microwave resonator, non-invasive detection, environmental effect elimination, switching circuit.



I. INTRODUCTION

DIABETES mellitus is a significant worldwide health problem due to various secondary diseases. Blood glucose levels higher than 230 mg/dL are called

Manuscript received February 4, 2020; revised March 27, 2020; accepted March 29, 2020. Date of publication April 1, 2020; date of current version July 6, 2020. This work was supported by the Basic Science Research Program through the National Research Foundation of Korea (NRF) funded by the Ministry of Science and ICT under Grant NRF-2017R1A2B2011724. The associate editor coordinating the review of this article and approving it for publication was Prof. Danilo Demarchi. (Corresponding author: Jong-Gwan Yook.)

Chorom Jang, Jin-Kwan Park, and Jong-Gwan Yook are with the Department of Electrical and Electronic Engineering, Yonsei University, Seoul 03722, South Korea (e-mail: chorom@yonsei.ac.kr; paladin91@yonsei.ac.kr; jgyook@yonsei.ac.kr).

Hee-Jo Lee is with the Department of Physics Education, College of Education, Daegu University, Daegu 38453, South Korea (e-mail: hjlee@daegu.ac.kr).

Gi-Ho Yun is with the Department of Information and Communication Engineering, Sungkyul University, Anyang 14097, South Korea (e-mail: ghyun@sungkyul.ac.kr).

Digital Object Identifier 10.1109/JSEN.2020.2984779

hyperglycemia [1]. If hyperglycemia persists, it causes many complications such as stroke, eye disease, renal failure, and diabetic foot [2], [3]. Another severe case, hypoglycemia, refers to a condition in which the blood glucose level is less than 65 mg/dL [4]. Hypoglycemia has a higher rate of mortality than hyperglycemia [5]. To avoid these dangerous conditions, diabetic patients take a blood sample from their fingertip using a lancet from a commercial blood glucose sensor several times a day [6]. This process of pricking a fingertip every day to monitor the blood glucose level is very painful for patients. To alleviate this affliction, various devices have been proposed to detect blood glucose levels via non-invasive methods. Thermal emission spectroscopy is a method for measuring the emitted infrared (IR) signals generated from the human body due to changes in blood glucose levels [7]. However, this method has limitations because it is affected by the ambient temperature and body movements. Another non-invasive method is Raman spectroscopy [8]. This method uses a laser

radiation source in the visible to mid-infrared (MIR) range and measures the light scattered from transparent samples. However, the instability of the laser intensity is a limitation. In addition, the need for a long spectral acquisition time limits the use of Raman spectroscopy. Ocular spectroscopy is another non-invasive method for glucose monitoring [9]. This method measures the glucose concentration in tears using a contact lens. The lens is illuminated with a light source, and the variation in the wavelength of the reflected light is measured. However, this method has several limitations such as biocompatibility, lifetime of the contact lens, discomfort, and a time delay between the tear and blood glucose levels.

On the other hand, the microwave method utilizes the penetrating capability of electromagnetic wave [10]–[16]. Among microwave devices, microwave resonators are advantageous for non-invasive detection because they store electromagnetic energy in the near-field region, where there is a strong electromagnetic field within a short distance. Moreover, they are reusable, portable, easy to fabricate and have low power consumption. Because of these advantages, non-invasive glucose sensors utilizing the microwave method have been proposed in recent decades [17]–[21]. However, microwave-based sensors are strongly affected by changes in temperature and other physical parameters [22]. Because the variations in the electrical properties of the blood glucose level as a function of the concentration are extremely small, these variations are highly obscured by small changes in other parameters, such as physical environmental parameters, including the ambient temperature and relative humidity. Thus, it is necessary to consider the effects of the surrounding environmental conditions to realize more practical and accurate detection. In an effort to alleviate this problem, a temperature correction function was derived to eliminate the detection error caused by ambient temperature fluctuations in our previous study [23]. However, this method calibrates out only the ambient temperature effect by utilizing a temperature correction function obtained from the response of the sensor. Thus, the effect of the ambient temperature is not removed in real time. The ambient temperature can also be corrected by precisely knowing the temperature at the time of the measurement. In addition, the derived temperature correction function has a limitation: it is only applicable to the proposed certain resonator.

In this paper, changes in the dielectric constant due to changes in the ambient temperature and relative humidity are analyzed. In addition, a complementary split ring resonator (CSRR) is designed to detect the glucose concentration; then, a fluidic glucose sensor based on dual CSRRs and a switching circuit is proposed to calibrate out the errors due to changes in the environmental conditions in real time. Moreover, the performance of the proposed sensor is verified by repeated measurements. It is demonstrated that glucose concentrations can be noninvasively and continuously detected by the proposed sensor under practical environmental conditions.

II. SENSOR DESIGN

A. Motivation for the Proposed Sensor

The accuracy of glucose level detection by the microwave technique is affected by environmental conditions [22]. It is

well known that the ambient temperature and relative humidity affect the dielectric constant of liquid and air, and these effects must be minimized because the detection of glucose concentrations with a microwave resonator is based on the detection of subtle changes in the dielectric constant of the analytes. With this motivation, the effects of the ambient temperature and relative humidity on DI water and air are analyzed, and a fluidic glucose sensor that eliminates the environmental effects is proposed in this paper.

1) *Environmental Effects on DI Water*: The frequency dependence of the permittivity of water is given by the Debye model as follows:

$$\varepsilon_{water} = \varepsilon_{\infty} + \frac{\varepsilon_s - \varepsilon_{\infty}}{1 - j(f/\gamma_D)} \quad (1)$$

where ε_s is the static permittivity of DI water and ε_{∞} is the optical permittivity at high frequency. γ_D is the electrical relaxation frequency. As the temperature increases, the hydrogen-bonded forces between H₂O molecules follow an exponential temperature law, and DI water has lower viscosity. Thus, the parameters in (1) are modified as follows [24]:

$$\varepsilon_{\infty} = 0.066 \cdot \varepsilon_s \quad (2)$$

and

$$\gamma_D = 20.1 \exp(7.88 \cdot \theta) \quad (3)$$

where

$$\theta = 1 - \frac{300}{T} \quad (4)$$

T is the ambient temperature in Kelvin. As shown in (1)–(4), the permittivity of DI water is affected by the ambient temperature.

2) *Environmental Effects on Air*: The permittivity of air is not frequency dependent, unlike that of DI water [25]. The permittivity of air, including the environmental parameters, is expressed as follows [26]:

$$\varepsilon_{air} = \varepsilon_0 \cdot \left[1 + \frac{211}{T} \cdot \left(P + \frac{48 \cdot P_s \cdot RH}{T} \right) \cdot 10^{-6} \right] \quad (5)$$

where ε_0 is the permittivity of vacuum (8.854×10^{-12}), RH is the relative humidity as a percentage (%), and P and P_s are the air pressure and saturated water vapor pressure in mmHg. The permittivity of air is affected by the ambient temperature, relative humidity and air pressure.

The ambient temperature affects both the permittivity of water and that of air, whereas the relative humidity affects only the permittivity of air. It is clear that the ambient temperature more significantly affects the glucose concentration detection than the relative humidity does.

B. Design of the Microwave Resonator

In recent decades, various glucose sensors in the microwave regime have been reported [27]–[32]. However, they are impractical because they are bulky and blood must be collected for actual use. Thus, planar microwave glucose sensors have been proposed [33]–[35]. A complementary split ring resonator (CSRR), which is a planar-type microwave resonator,

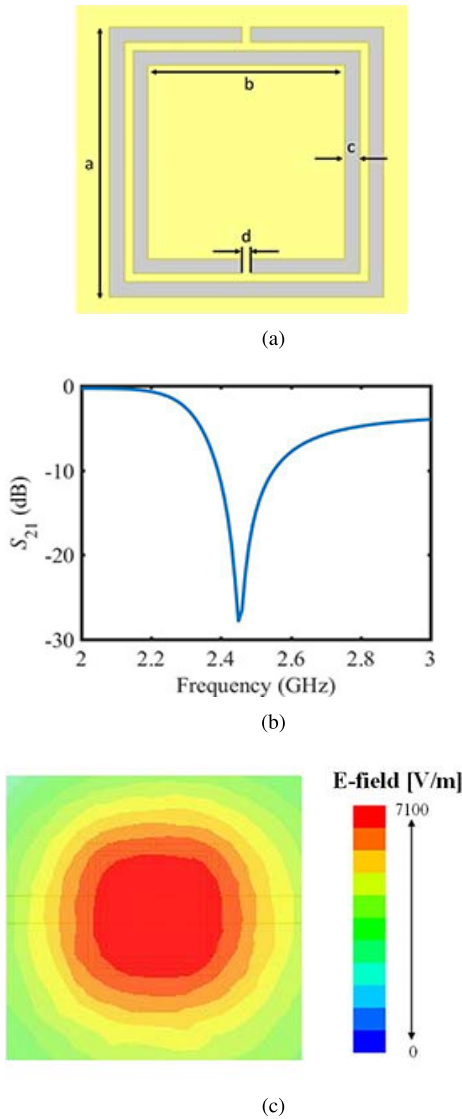


Fig. 1. Design and simulation of the complementary split ring resonator (CSRR) (a) Double split ring of the designed CSRR. ($a = 7.9$ mm, $b = 5.94$ mm, $c = 0.38$ mm, and $d = 0.2$ mm). (b) Transmission coefficient of the CSRR. (c) Electric field distribution.

is widely used for material characterization due to the strongly formed electromagnetic field and high sensitivity [36]. In a CSRR, the ground plane of the microstrip line is etched in the form of double square rings with a gap. Resonance of the CSRR occurs by the inductive and capacitive components of the double split ring and the capacitance between the signal line and the ground plane. Thus, the resonant frequency of the CSRR is determined as follows [37]:

$$f_r = \frac{1}{2\pi\sqrt{L_r(C + C_r)}} \quad (6)$$

where L_r and C_r are the inductance and capacitance of the double split ring, respectively. C is the capacitance between the signal line and the ground plane. The double split ring of the designed CSRR is shown in Fig. 1(a). The transmission characteristic of the designed CSRR is -28 dB at 2.45 GHz, which is in the ISM band, as shown in Fig. 1(b). Detection using microwave resonators basically utilizes changes in their characteristics due to the interaction between the

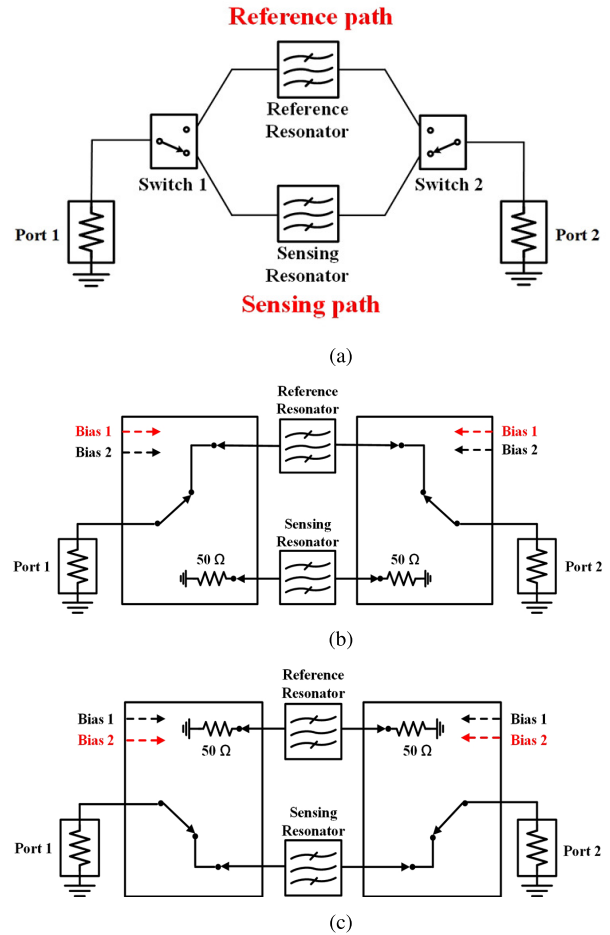


Fig. 2. Configuration of proposed sensor. (a) Schematic. (b) Operation of reference path. (c) Operation of sensing path.

electromagnetic field and the analytes. It is demonstrated that a higher-intensity electromagnetic field improves the sensitivity. Thus, based on the electric field distribution obtained by simulation, as shown in Fig. 1(c), the effective sensing region is determined to be the center of the double split ring, where the electric field is the strongest.

C. Configuration of the Proposed Sensor

Based on the previous section, the elimination of environmental effects is clearly necessary to detect the glucose concentration using a microwave resonator. The configuration of the proposed sensor for environmental effect elimination is shown in Fig. 2(a). Two identical CSRRs are employed for calibrating out the errors due to environmental effects. One of the two CSRRs detects only environmental conditions, acting as a reference resonator, while the other sensing resonator detects both the environmental conditions and the glucose concentration. It is assumed that identical CSRRs exhibit identical frequency characteristics as a function of ambient temperature and relative humidity variations. Note that these two CSRRs are located sufficiently far from each other so that there is no interference between them. Moreover, two RF switches are connected to both ends of the resonators to decrease the number of RF ports and improve the isolation

between the two resonators. In addition, the cost of measurement can be reduced by decreasing the number of ports. For error correction in real time, the signal path is alternately determined using two switches by simultaneously supplying a bias every 0.5 sec. When a bias 1 is high and bias 2 is low, the reference path is selected as shown in Fig. 2(b), and the transmission coefficient of reference resonator is measured. After 0.5 second, the bias 1 and bias 2 are changed to low and high, respectively. Then the sensing path is selected as shown in Fig. 2(c) and the transmission coefficient of sensing resonator is measured. The environmental effect elimination can be conducted by calculating the differences between the transmission coefficients of reference and sensing resonators every second. This process is repeated for the continuous monitoring.

To characterize the performance of the proposed sensor, the transmission coefficient is mathematically analyzed. The assumed experimental conditions are that the fluidic channel that contains the glucose solution passes over the resonator while the ambient temperature, relative humidity and glucose concentration are varied. Then, the amplitude and phase components of the transmission coefficient of the CSRR with the fluidic channel are modulated by the time-varying components as follows:

$$\begin{aligned} S_{21,sensor} &= |A_{sensor}| \cdot e^{j(\angle A_{sensor})} \\ &= |A_{fixed}| \cdot |1 + \tau_{varying}| \cdot e^{j(\angle A_{fixed} + \angle \tau_{varying})} \\ &= |A_{CSRR}| \cdot |1 + \tau_T(t)| \cdot |1 + \tau_{RH}(t)| \cdot |1 + \tau_{glu}(t)| \\ &\quad \cdot e^{j(\angle A_{CSRR} + \angle \tau_T(t) + \angle \tau_{RH}(t) + \angle \tau_{glu}(t))} \end{aligned} \quad (7)$$

where $|A_{sensor}|$ is the amplitude of the transmission coefficient, which is composed of a fixed signal and time-varying signals. The fixed signal value is the transmission coefficient of the CSRR with the fluidic channel that contains deionized (DI) water (A_{CSRR}). The time-varying signals contain information on the ambient temperature (τ_T), relative humidity (τ_{RH}) and glucose concentration (τ_{glu}). Because the amplitude and phase variations due to the changes in the glucose level are very small, they can be considered as a narrowband modulation, and (5) can be simplified as follows [38]:

$$\begin{aligned} S_{21,sensor} &= |A_{CSRR}| \cdot |1 + \tau_T(t)| \cdot |1 + \tau_{RH}(t)| \cdot |1 + \tau_{glu}(t)| \\ &\quad \cdot [1 + j(\angle \tau_{glu})] \cdot e^{j(\angle A_{CSRR} + \angle \tau_T(t) + \angle \tau_{RH}(t))} \end{aligned} \quad (8)$$

From (6), note that the ambient temperature and relative humidity lead to amplitude and phase modulations, whereas the glucose concentration leads to only amplitude modulation. τ_{glu} can be considered a constant, and the transmission coefficient can be expressed as follows:

$$\begin{aligned} S_{21,sensor} &= |A_{CSRR}| \cdot |1 + \tau_T(t)| \cdot |1 + \tau_{RH}(t)| \cdot |1 + \tau_{glu}(t)| \\ &\quad \cdot e^{j(\angle A_{CSRR} + \angle \tau_T(t) + \angle \tau_{RH}(t))} \end{aligned} \quad (9)$$

When this result is applied to the reference resonator, which detects only environmental conditions, it can be expressed as follows:

$$\begin{aligned} S_{21,ref} &= |A_{CSRR}| \cdot |1 + \tau_T(t)| \cdot |1 + \tau_{RH}(t)| \\ &\quad \cdot e^{j(\angle A_{CSRR} + \angle \tau_T(t) + \angle \tau_{RH}(t))} \end{aligned} \quad (10)$$

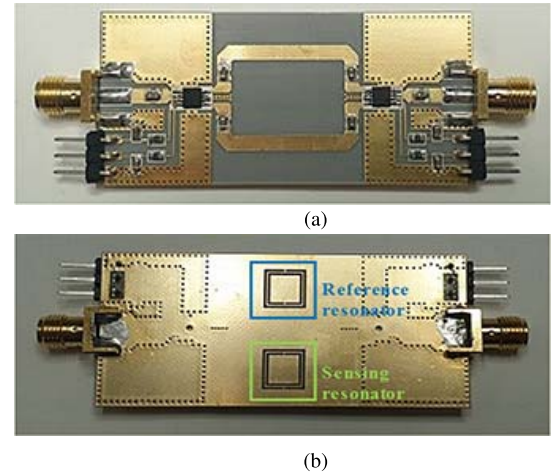


Fig. 3. Photograph of the fabricated sensor. (a) Top view. (b) Bottom view.

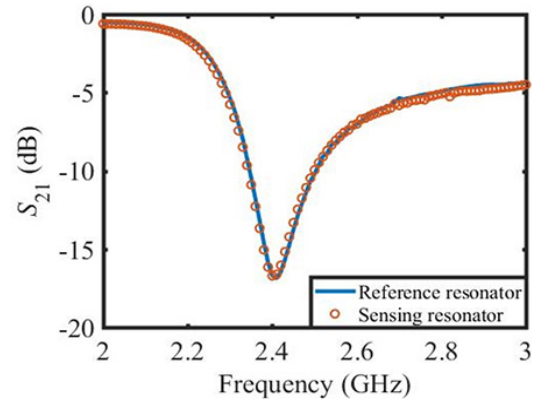


Fig. 4. Transmission coefficient of the reference resonator and sensing resonator.

Then, the transmission coefficient due to the variation in the glucose concentration can be calculated as follows:

$$S_{21,glucose} = S_{21,sensor} / S_{21,ref} \quad (11)$$

D. Fabrication of the Sensor and Experimental Setup

The proposed CSRR is fabricated by photolithography and a chemical etching process, as shown in Fig. 3(a) and (b). The substrate of the proposed sensor is Neltec NY9217(IM), which has a dielectric constant of 2.17, a dielectric loss ($\tan\delta$) of 0.0008, and a thickness of 0.8 mm. A fluidic channel of PTFE (polytetrafluoroethylene) with a permittivity of 2.1 and a loss tangent of 0.001 is prepared. The inner and outer diameters are 1/32 in and 1/16 in, respectively. The fluidic channel containing the glucose solution is loaded such that it passes over the center of the double split ring, which was determined to be the effective sensing region in the previous section. Thus, the volume of the sample in the effective sensing region is approximately $3.9 \mu\ell$. To verify the identical characteristics of the two resonators, the transmission coefficient is measured using a vector network analyzer with a bias on the switches. The measured transmission coefficient of each path is plotted in Fig. 4 when the fluidic channel is loaded on the sensing region. Because of the high dielectric constant and dielectric loss of the DI water in the fluidic

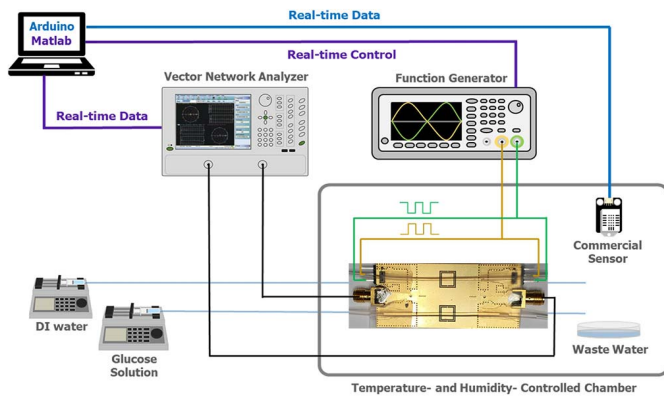


Fig. 5. Experimental setup for the measurement.

channel, the resonant frequency is shifted to 2.42 GHz, and the transmission coefficient changes to -16.8 dB.

The experimental setup is illustrated in Fig. 5. The fabricated sensor is located in a temperature- and humidity-controlled chamber for the environmental condition tests. To measure the transmission coefficient of the proposed sensor, the connectors at both ends of the sensor are linked to the vector network analyzer (MS4647B). A bias is simultaneously supplied to the two RF switches using a two-channel function generator (33510B) to select a signal path. The outputs of channel 1 and channel 2 of the function generator generate square waveforms complementary to each other every second, as shown in Fig. 5. This setup enables the reference resonator and sensing resonator to be alternately activated every second, and the environmental effects are calibrated out in real time. The vector network analyzer is connected to a laptop for data acquisition, and the function generator is connected for waveform control in real time. Commercial temperature and humidity sensors are used to acquire environmental data in real time. The analytes are prepared with five different glucose concentrations (0, 100, 200, 300, and 400 mg/dL) to consider the possible blood glucose levels of the human body. Two syringe pumps and fluidic channels are used to noninvasively detect the analytes. The flow rates of the two syringe pumps are set to $200 \mu\text{l}/\text{min}$. Because the sensing resonator of the proposed sensor is designed to respond to both environmental conditions and glucose concentration changes, a fluidic channel filled with the analytes is loaded on top of the sensing resonator. In contrast, the reference resonator is designed to respond to only environmental changes, so a reference fluidic channel filled with DI water is loaded onto the reference resonator. The ambient temperature inside the temperature- and humidity-controlled chamber is set to increase from 293 K to 313 K with a step of 5 K to consider room temperature and body temperature, while the relative humidity is set to increase from 30% to 90% with a step of 15%. The transmission coefficient of the proposed sensor is continuously measured at 2.42 GHz, which is the resonant frequency of the CSRR loaded with the fluidic channel containing DI water.

III. EXPERIMENTAL RESULTS

To quantify the performance of the proposed sensor, the transmission coefficient of the sensor is measured

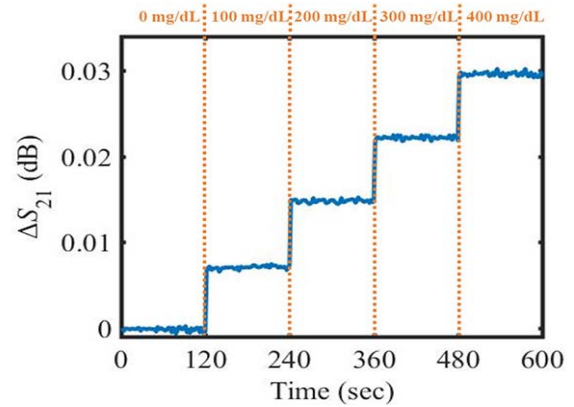


Fig. 6. Variation in the transmission coefficient under constant temperature and relative humidity conditions.

TABLE I
AMBIENT TEMPERATURE AND RELATIVE HUMIDITY SETTING FOR THE ENVIRONMENTAL EFFECT ELIMINATION

Time (sec)	Glucose Concentration (mg/dL)	Ambient Temperature (K)	Relative Humidity (%)
0-120	0	303	60
120-240	100	298	75
240-360	200	293	90
360-480	300	308	45
480-600	400	313	30

under well-controlled conditions with an ambient temperature of 303 K and a relative humidity of 60%. Furthermore, the glucose concentration is increased every 2 minutes. The variation in the transmission coefficient when the glucose concentration varies from 0 to 400 mg/dL is measured as approximately 0.03 dB, as shown in Fig. 6. In addition, to quantify the effects of the ambient temperature and relative humidity compared to the glucose concentration, the transmission coefficient is measured over each condition range of the glucose concentration, ambient temperature, and relative humidity. The variation in the transmission coefficient due to the glucose concentration is approximately 0.03 dB, that due to the ambient temperature is approximately 2.5 dB, and that due to the relative humidity is approximately 0.25 dB, as shown in Fig. 7(a) and (b). Based on these results, the variation in the transmission coefficient due to the glucose concentration changes is clearly an order of magnitude smaller than those due to the ambient temperature and relative humidity changes. Therefore, environmental effects must be eliminated to accurately detect glucose levels. Note that the ambient temperature is more influential than the relative humidity, as shown in Fig. 7(c).

To verify the environmental effect elimination ability in real time, the glucose level is detected under arbitrarily varied environmental conditions. The random settings of the ambient temperature and relative humidity are shown in Table I. The variation in the transmission coefficient when the environmental effects are not eliminated using only the sensing resonator is shown in Fig. 8. In this figure, because the ambient temperature has the strongest impact on the transmission coefficient of the sensor, the change in the transmission coefficient has

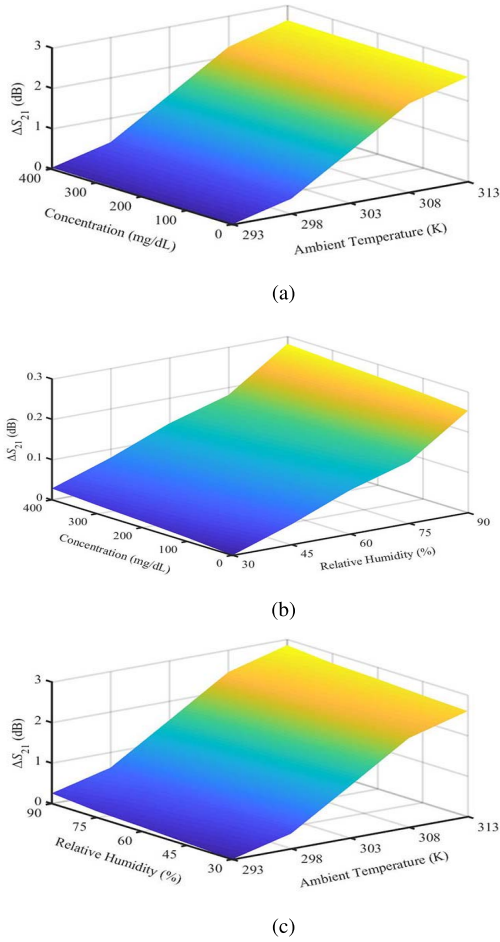


Fig. 7. 3D graph to verify the environmental effects. (a) Variation in the transmission coefficient due to the glucose concentration and ambient temperature. (b) Variation in the transmission coefficient due to the glucose concentration and relative humidity. (c) Variation in the transmission coefficient due to the ambient temperature and relative humidity.

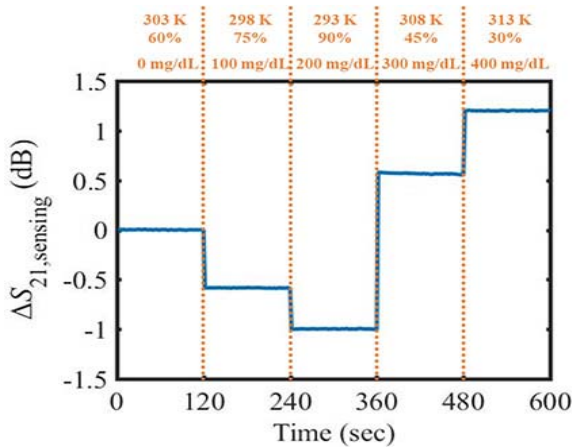


Fig. 8. Variation in the transmission coefficient of the sensing resonator when the environmental effect is not eliminated.

an identical trend to the change in the ambient temperature regardless of the increase in the glucose concentration. From (11), the environmental effects in the dB scale can be eliminated as follows:

$$\Delta S_{21,glucose}(dB) = \Delta S_{21,sensing}(dB) - \Delta S_{21,ref}(dB), \quad (12)$$

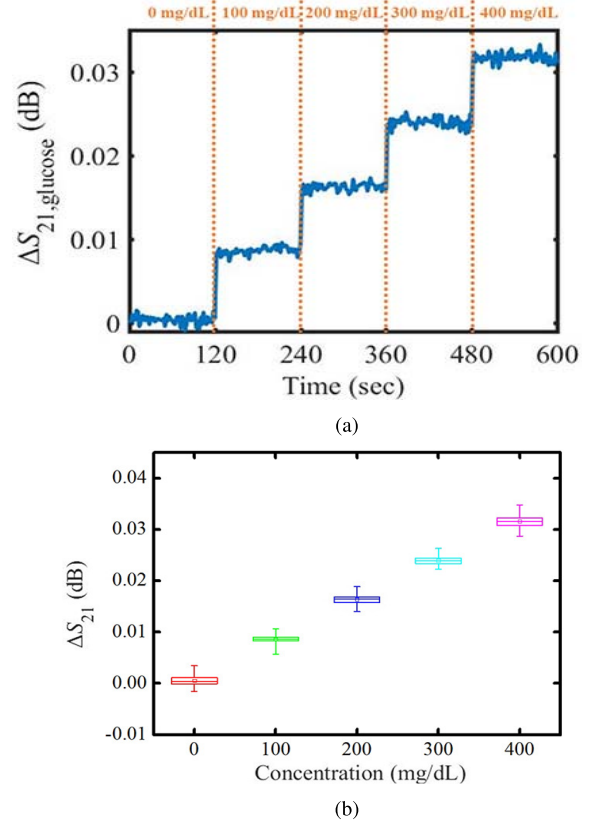


Fig. 9. Results of environmental effect elimination. (a) Variation in the transmission coefficient after environmental effect elimination. (b) Statistical results of the proposed sensor.

TABLE II
MEAN VALUES OF THE STATISTICAL DATA DISTRIBUTION

Glucose concentration (mg/dL)	Mean value (dB)
0	0.001
100	0.009
200	0.016
300	0.024
400	0.032

where $\Delta S_{21,glucose}$ is the variation in the transmission coefficient after environmental effect elimination and $\Delta S_{21,ref}$ is the variation in the transmission coefficient of the reference resonator. The variation in the transmission coefficient due to only the glucose concentration after elimination of the environmental effects is shown in Fig. 9(a). This figure clearly demonstrates that the glucose concentration can be detected with the proposed calibration methodology. Fig. 9(b) shows the statistical results of repeated measurements with 360 samples. The bars outside the boxes show the maximum and minimum values, and the bounds of the boxes indicate the 25 and 75 percentiles of the data distribution. The lines and squares inside the boxes represent the median and mean values of the data, respectively. The boxes do not overlap, and the glucose concentration can be clearly discriminated from the variation in the transmission coefficient. The mean values of the statistical data distributions are summarized in Table II. It is demonstrated in this work that the clinically meaningful

glucose concentration can be noninvasively detected by measuring the change in the transmission coefficient of the proposed sensor system.

IV. CONCLUSION

In this paper, a novel fluidic glucose sensor with environmental effect elimination based on two identical CSRRs and a switching circuit is proposed for non-invasive measurement. The two identical CSRRs consist of a reference resonator, which detects environmental changes, and a sensing resonator, which detects both environmental conditions and glucose concentration changes. It is verified that changes in environmental factors, such as the ambient temperature and relative humidity, much more strongly influence the transmission characteristics than changes in the glucose concentration. For more practical and accurate detection, the environmental effects are eliminated in real time by comparing the signals from the two resonators. The variation in the transmission coefficient of the proposed sensor is approximately 0.03 dB when the glucose concentration is increased from 0 to 400 mg/dL, and this performance is consistent with the measurement data under constant environmental conditions. Thus, it is clearly demonstrated that the proposed sensor can noninvasively and continuously detect the glucose concentration under practical environmental conditions. Future works will focus on advanced research such as enhancement of the sensitivity, state of hydrogenation of the patients, and analysis of human tissue and blood plasma. Moreover, enhancement of the selectivity and in vivo testing of the advanced sensor will be performed.

REFERENCES

- [1] C. H. Wei and S. E. Litwin, "Hyperglycemia and adverse outcomes in acute coronary syndromes: Is serum glucose the provocateur or innocent bystander?" *Diabetes*, vol. 63, no. 7, pp. 2209–2212, Jul. 2014.
- [2] K. M. V. Narayan and U. P. Gujral, "Evidence tips the scale toward screening for hyperglycemia," *Diabetes Care*, vol. 38, no. 8, pp. 1399–1401, Aug. 2015.
- [3] G. E. Umpierrez and F. J. Pasquel, "Management of inpatient hyperglycemia and diabetes in older adults," *Diabetes Care*, vol. 40, no. 4, pp. 509–517, Apr. 2017.
- [4] S.-W. Yi, S. Park, Y.-H. Lee, B. Balkau, and J.-J. Yi, "Fasting glucose and all-cause mortality by age in diabetes: A prospective cohort study," *Diabetes Care*, vol. 41, no. 3, pp. 623–626, Mar. 2018.
- [5] C. Desouza, H. Salazar, B. Cheong, J. Murgu, and V. Fonseca, "Association of hypoglycemia and cardiac ischemia: A study based on continuous monitoring," *Diabetes Care*, vol. 26, no. 5, pp. 1485–1489, May 2003.
- [6] D. Bruen, C. Delaney, L. Florea, and D. Diamond, "Glucose sensing for diabetes monitoring: Recent developments," *Sensors*, vol. 17, no. 8, p. 1866, 2017.
- [7] S.-J. Yeh, C. F. Hanna, and O. S. Khalil, "Monitoring blood glucose changes in cutaneous tissue by temperature-modulated localized reflectance measurements," *Clin. Chem.*, vol. 49, no. 6, pp. 924–934, Jun. 2003.
- [8] A. Berger, "Feasibility of measuring blood glucose concentration by near-infrared Raman spectroscopy," *Spectrochimica Acta A, Mol. Spectrosc.*, vol. 53, no. 2, pp. 287–292, Feb. 1997.
- [9] A. Domschke, W. F. March, S. Kabilan, and C. Lowe, "Initial clinical testing of a holographic non-invasive contact lens glucose sensor," *Diabetes Technol. Therapeutics*, vol. 8, no. 1, pp. 89–93, Feb. 2006.
- [10] J.-K. Park, T.-G. Kang, B.-H. Kim, H.-J. Lee, H. H. Choi, and J.-G. Yook, "Real-time humidity sensor based on microwave resonator coupled with PEDOT: PSS conducting polymer film," *Sci. Rep.*, vol. 8, no. 1, p. 439, Dec. 2018.
- [11] H.-J. Lee, J.-H. Lee, S. Choi, I.-S. Jang, J.-S. Choi, and H.-I. Jung, "Asymmetric split-ring resonator-based biosensor for detection of label-free stress biomarkers," *Appl. Phys. Lett.*, vol. 103, no. 5, Jul. 2013, Art. no. 053702.
- [12] J.-K. Park *et al.*, "Noncontact RF vital sign sensor for continuous monitoring of driver status," *IEEE Trans. Biomed. Circuits Syst.*, vol. 13, no. 3, pp. 493–502, Jun. 2019.
- [13] W. Liu, M. Wang, and Y. Shi, "A transmission-reflection method for complex permittivity measurement using a planar sensor," *IEEE Sensors J.*, vol. 18, no. 10, pp. 4059–4065, May 2018.
- [14] J.-M. Boccard, T. Aftab, J. Hoppe, A. Yousaf, R. Hutter, and L. M. Reindl, "High-resolution, far-field, and passive temperature sensing up to 700 °C using an isolated ZST microwave dielectric resonator," *IEEE Sensors J.*, vol. 16, no. 3, pp. 715–722, Feb. 2016.
- [15] E. L. Chuma, Y. Iano, G. Fontgalland, and L. L. Bravo Roger, "Microwave sensor for liquid dielectric characterization based on metamaterial complementary split ring resonator," *IEEE Sensors J.*, vol. 18, no. 24, pp. 9978–9983, Dec. 2018.
- [16] P. Velez, L. Su, K. Grenier, J. Mata-Contreras, D. Dubuc, and F. Martin, "Microwave microfluidic sensor based on a microstrip splitter/combiner configuration and split ring resonators (SRRs) for dielectric characterization of liquids," *IEEE Sensors J.*, vol. 17, no. 20, pp. 6589–6598, Oct. 2017.
- [17] J. Kim, A. Babajanyan, A. Hovsepyan, K. Lee, and B. Friedman, "Microwave dielectric resonator biosensor for aqueous glucose solution," *Rev. Sci. Instrum.*, vol. 79, no. 8, Aug. 2008, Art. no. 086107.
- [18] P. Velez, J. Mata-Contreras, D. Dubuc, K. Grenier, and F. Martin, "Solute concentration measurements in diluted solutions by means of split ring resonators," in *Proc. 48th Eur. Microw. Conf. (EuMC)*, Sep. 2018, pp. 231–234.
- [19] S. Y. Huang *et al.*, "Microstrip line-based glucose sensor for noninvasive continuous monitoring using the main field for sensing and multivariable crosschecking," *IEEE Sensors J.*, vol. 19, no. 2, pp. 535–547, Jan. 2019.
- [20] V. Turgul and I. Kale, "Simulating the effects of skin thickness and fingerprints to highlight problems with non-invasive RF blood glucose sensing from fingertips," *IEEE Sensors J.*, vol. 17, no. 22, pp. 7553–7560, Nov. 2017.
- [21] G. Govind and M. J. Akhtar, "Metamaterial-inspired microwave microfluidic sensor for glucose monitoring in aqueous solutions," *IEEE Sensors J.*, vol. 19, no. 24, pp. 11900–11907, Sep. 2019.
- [22] S. K. Vashist, "Non-invasive glucose monitoring technology in diabetes management: A review," *Analytica Chim. Acta*, vol. 750, pp. 16–27, Oct. 2012.
- [23] C. Jang, J.-K. Park, H.-J. Lee, G.-H. Yun, and J.-G. Yook, "Temperature-corrected fluidic glucose sensor based on microwave resonator," *Sensors*, vol. 18, no. 11, p. 3850, 2018.
- [24] H. J. Liebe, G. A. Hufford, and T. Manabe, "A model for the complex permittivity of water at frequencies below 1 THz," *Int. J. Infr. Millim. Waves*, vol. 12, no. 7, pp. 659–675, Jul. 1991.
- [25] J. A. Huisman, W. Bouten, J. A. Vrugt, and P. A. Ferré, "Accuracy of frequency domain analysis scenarios for the determination of complex dielectric permittivity," *Water Resour. Res.*, vol. 40, no. 2, Feb. 2004, Art. no. W02401.
- [26] N. Lea, "Notes on the stability of LC oscillators," *J. Inst. Elect. Eng. III, Radio Commun. Eng.*, vol. 92, no. 20, pp. 261–274, Dec. 1945.
- [27] S. Kim *et al.*, "Noninvasive in vitro measurement of pig-blood d-glucose by using a microwave cavity sensor," *Diabetes Res. Clin. Pract.*, vol. 96, no. 3, pp. 379–384, Jun. 2012.
- [28] V. Turgul and I. Kale, "Characterization of the complex permittivity of glucose/water solutions for noninvasive RF/microwave blood glucose sensing," in *Proc. IEEE Int. Instrum. Meas. Technol. Conf. Proc.*, May 2016, pp. 1–5.
- [29] A. Babajanyan, H. Melikyan, S. Kim, J. Kim, K. Lee, and B. Friedman, "Real-time noninvasive measurement of glucose concentration using a microwave biosensor," *J. Sensors*, vol. 2010, pp. 1–7, Jun. 2010.
- [30] Y. Fan, X. Deng, Q. Wang, and W. Wang, "Testing glucose concentration in aqueous solution based on microwave cavity perturbation technique," in *Proc. 3rd Int. Conf. Biomed. Eng. Informat.*, Oct. 2010, pp. 1046–1049.
- [31] C. Jang, J.-K. Park, G.-H. Yun, and J.-G. Yook, "Noninvasive method to distinguish between glucose and sodium chloride solution using complementary split-ring resonator," *J. Korean Inst. Electromagn. Eng. Sci.*, vol. 29, no. 4, pp. 247–255, Apr. 2018.
- [32] G.-H. Yun, "A study on slot coupled capacitor resonator for non-invasive glucose monitoring in earlobe," *J. Korean Inst. Electromagn. Eng. Sci.*, vol. 28, no. 4, pp. 279–285, Apr. 2017.
- [33] B. R. Jean, E. C. Green, and M. J. McClung, "A microwave frequency sensor for non-invasive blood-glucose measurement," in *Proc. IEEE Sensors Appl. Symp.*, Feb. 2008, pp. 4–7.

- [34] H. Choi, J. Nylon, S. Luzio, J. Beutler, and A. Porch, "Design of continuous non-invasive blood glucose monitoring sensor based on a microwave split ring resonator," in *Proc. IEEE MTT-S Int. Microw. Workshop Ser. RF Wireless Technol. for Biomed. Healthcare Appl. (IMWS-Bio)*, Dec. 2014, pp. 1–3.
- [35] T. Chretiennot, D. Dubuc, and K. Grenier, "Microwave-based microfluidic sensor for non-destructive and quantitative glucose monitoring in aqueous solution," *Sensors*, vol. 16, no. 10, p. 1733, 2016.
- [36] C.-S. Lee and C.-L. Yang, "Complementary split-ring resonators for measuring dielectric constants and loss tangents," *IEEE Microw. Wireless Compon. Lett.*, vol. 24, no. 8, pp. 563–565, Aug. 2014.
- [37] M. S. Boybay and O. M. Ramahi, "Material characterization using complementary split-ring resonators," *IEEE Trans. Instrum. Meas.*, vol. 61, no. 11, pp. 3039–3046, Dec. 2012.
- [38] Y.-J. An, G.-H. Yun, and J.-G. Yook, "Sensitivity enhanced vital sign detection based on antenna reflection coefficient variation," *IEEE Trans. Biomed. Circuits Syst.*, vol. 10, no. 2, pp. 319–327, Apr. 2016.



Chorom Jang (Student Member, IEEE) was born in Incheon, South Korea. She received the B.S. degree in electronic engineering from Seokyeong University, Seoul, South Korea, in 2017. She is currently pursuing the Ph.D. degree in electrical and electronics engineering with Yonsei University, Seoul. Her main research interests are RF-based sensors such as glucose, vital-sign, and pressure sensors, and microwave components/systems.



Jin-Kwan Park (Student Member, IEEE) was born in Seoul, South Korea. He received the B.S. degree in electronics and electrical engineering from Dongguk University, Seoul, in 2014. He is currently pursuing the Ph.D. degree in electrical and electronics engineering with Yonsei University, Seoul. His main research interests are RF-based sensors, such as vital-sign, humidity, glucose, and gas sensors, and microwave/millimeter-wave components/systems.



Hee-Jo Lee (Member, IEEE) received the Ph.D. degree in electrical and electronic engineering from Yonsei University, Seoul, South Korea, in 2010. From March 2010 to March 2012, he worked as a Postdoctoral Researcher in electrical and electronic engineering with Yonsei University, and the Graphene Research Institute, Sejong University, Seoul. From April 2012 to August 2014, he worked as a Research Professor in mechanical engineering, electrical, and electronic engineering with Yonsei University. Since September 2014, he has been an Assistant Professor with the Department of Physics Education, Daegu University. His main research interests are in the areas of electromagnetic wave and field theory, RF/microwave bio and gas-sensors, RF/microwave circuit modeling, and characterization of carbon nanomaterials, including graphene, graphene ribbon, and graphene oxide, and electromagnetic metamaterials for biosensing.



Gi-Ho Yun was born in Jeonju-Si, South Korea. He received the M.S. and Ph.D. degrees in electronics engineering from Yonsei University, Seoul, South Korea, in 1986 and 1999, respectively. From 1985 to 1997, he was with Samsung Electronics and Samsung Electro-Mechanics. He was with Honam University, Gwangju, South Korea, from 1997 to 2008. He is currently a Professor with the Division of Information and Communication Engineering, Sungkyul University, Anyang, South Korea. He is also with the Advanced Computational Electromagnetic Laboratory, Yonsei University. His current research interests include the areas of active and passive circuitry in the RF/MW frequency and various sensors to detect vital signals and biosignals in the human body.



Jong-Gwan Yook (Senior Member, IEEE) was born in Seoul, South Korea. He received the B.S. and M.S. degrees in electronics engineering from Yonsei University, Seoul, in 1987 and 1989, respectively, and the Ph.D. degree from the University of Michigan, Ann Arbor, MI, USA, in 1996. He is currently a Professor with the School of Electrical and Electronic Engineering, Yonsei University. His main research interests are in the areas of theoretical/numerical electromagnetic modeling and characterization of microwave/millimeter-wave circuits and components, design of radio frequency integrated circuits (RFICs) and monolithic microwave integrated-circuits (MMICs), and analysis and optimization of high-frequency high-speed interconnects, including the signal/power integrity (EMI/EMC), based on frequency- and time-domain full-wave methods. Recently, his research team has developed various biosensors, such as carbon nanotube RF biosensors for nanometer-size antigen-antibody detection and remote wireless vital signal monitoring sensors.